Journal of Metals, Materials and Minerals, Vol.22 No.2 pp.105-117, 2012

Study of dynamic vulcanized PLA/ENR TPV filled with various organic modified MMT (OMMT)

Chanchai THONGPIN[1*], Nattakarn KUTTANATE[1], Kobchok KAMPUANG[1] and Nipa SUWANWANIT[1]

[1]Materials Science and Engineering Department, Faculty of Engineering and Industrial Technology, Silpakorn University, Sanamchandra Palace Campus, Nakornpathom, 73000, Thailand.

Abstract

In this research, we investigated the crystallization behavior of PLA and properties of PLA/ENR thermoplastic vulcanizates (TPVs). ENR was compounded with phenolic resin and with PLA at the blend ratio of 40/60 by using an internal mixer at 170°C and rotor speed of 70 rpm. Three types of organic modified montmorillonite (OMMT) which are Cloisite® 15A, Cloisite® 20 A and Cloisite® 30B were also added at various contents during mixing. The TPVs were pressed to form thin film in a compression molding machine and cooled down under pressure for 10 minutes. Crystallization behavior, thermal properties and morphology of TPVs were investigated using DSC, TGA and SEM, respectively. On the first heating, cold crystallization temperature (T_{cc}) of PLA, in the TPVs both with and without OMMT, was clearly occurred at lower temperature than that of the neat PLA. The melting temperature (T_m) of neat PLA exhibits 2 melting temperatures, i.e. T_{m1} and T_{m2}, as well as those in the TPVs. The crystallinity of PLA was found to be increased with the present of ENR. This confirmed the crystallization of PLA having ENR as nucleating agent. In this case crystallization of PLA during cooling could also be observed. On the second heating scan, the well defined T_g, T_{m1} and T_{m2} could be observed. The crystallinity of PLA of all TPVs was also considerably increased accept for TPV without OMMT where T_g and T_{ms} are slightly lowered by the degradation during heat experience, clarified by onset of degradation temperature (T_d). The addition of OMMT was found to enhance both crystallization behavior and thermal stability.

The research shows that types and content of OMMT did not much affect T_g and melting behavior of PLA but they affected crystallization behavior of PLA through sharpening cold crystallization peak and reducing cold crystallization temperature. In addition, there was a small exothermic peak during cooling. All types of organoclay could improve thermal stabilities of TPVs similarly. Especially, the presence of 3 and 5 phr of organoclay could compensate for lost thermal stabilities of TPVs satisfactorily.

Key words: PLA/ENR TPV, PLA crystallization, PLA/ENR TPV filled with OMMT.

Introduction

Recently, biopolymers have gained much interest as they can degrade and do not cause waste disposal problems. Thus, biopolymer is an alternative to petroleum based polymeric materials.

One of these biomaterials is the poly(lactic acid) (PLA) which is derived from biomass such as sugar, corn and beet. It is highly brittle and has poor crystallization behavior. To improve toughness and flexibility, rubber was blended with PLA.

Thermoplastic vulcanizates (TPVs) are materials prepared by mixing thermoplastic and rubber at high shear stress and temperature. The curing of rubber could occur during melt mixing and will be called dynamic vulcanization. From this process, cured rubber will be dispersed in the continuous thermoplastic matrix. Thus the properties of the materials will be the integration between easy processing like thermoplastic and elastomeric properties of rubber.(1)

To improve the properties of TPVs, clays were used as reinforcing agent. Clays are cheap and have good compatibility with polymer composites such as rubber, plastic, coating, color and etc. Since clays are hydrophilic but polymers almost are hydrophobic, they are generally not compatible.(2) Thus, it is necessary to modify the surface of clays

*Corresponding author E-mail: address: chanchai@su.ac.th

in order to improve the compatibility between clays and polymer matrix. Types of modifier and clay content are known to greatly affect the final properties of the composite. This research therefore aimed to study the effect of organically modified montmorillonite (OMMT) on thermal, morphology and mechanical properties of biopolymer/rubber thermoplastic vulcanizate.

The objective of this work was to improve toughness of PLA using epoxidized natural rubber (ENR) compound. The TPV obtained will be advantageous in terms of being biodegradable TPV. To improve the properties of TPV, various types of OMMT will be added.

Materials and Experimental Procedure

Materials

The PLA used in this study was supplied by NatureWorks LLC. The OMMTs (Closite® 15A, Closite® 20A, Closite® 30B) were supplied by Southern Clay Products, lnc. The structures of the OMMT are shown below. Epoxidized natural rubber (ENR) in this study was 50% epoxidation (ENR-50). Reactive phenolic resin was kindly donated by the Prince of Songkla University.

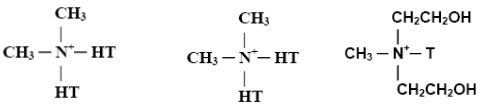

Cloisite®15A Cloisite®20A Closite®30B

Modifier concentration is at 125, 95 and 90 meq/100g MMT
T is Tallow (~65% C18, ~30%C16, ~5%C14

Sample Preparation

ENR was compounded with 5 phr of phenolic resin and 1, 3 and 5 phr of organoclay by internal mixer (MX105-D40L50, Chareon Tut Co., Ltd.). The concentration of organoclay stated was the actual concentration in TPVs. After ENR compound was prepared, its cure characteristic properties were tested using moving die rheometer (MDR) (GT-M2000, GOTECH TESTING MACHINES INC.). PLA was mixed with ENR compound in the internal mixer with the weight ratio of PLA 60:ENR compound 40. All samples were prepared by melt processing at 170°C. The mixing scheme was as followed: PLA pellets were firstly put in the internal mixer at rotor speed of 50 rpm. After PLA pellets started melting, rubber compound was put and the rotor speed was adjusted to 70 rpm. Melt processing was proceeded for 15 minutes.

The OMMT-PLA/ENR was also prepared in the same manner. The blends were compressed to form films (15x15x0.025 cm) by compression molding at 170°C by preheating the compound for 3 minutes and followed by compressing for 6 minutes. After that, the film was cooled to room temperature while being kept in the compressed mold.

Morphology Investigation

X-ray Diffraction (XRD; Bruker AXS D8) was used to study the dispersion of organoclays in TPVs. The samples was scanned in the range of 2-10°. An XRD diffractogram (intensity·2θ) was obtained from the analysis. The *d*-spacing (*d*) of the interlayer gallery was calculated using Bragg's law equation (as shown in Eq. (1)).

$$n\lambda = 2d\sin\theta \qquad (1)$$

The fractured surface of OMMT-PLA/ENR TPVs obtained from tensile test and failure in liquid nitrogen was coated with gold in vacuum. Then, SEM (JEOL JSM-5410, Faculty of Science, Silpakorn University) was used to investigate morphology of the composites.

Thermal Property Investigation

Thermal degradation behaviors were studied by the loss of weight from thermal degradation in TGA (TGA/DSC1 Module, METLER TOLEDO (Thailand) Co., Ltd.). The sample of OMMT-PLA/ ENR TPV around 5-10 mg was heated from 30 – 700°C with heating rate at 10°C/minutes.

The samples of OMMT-PLA/ENR TPV around 5-10 mg were put in aluminum pan. Then, test was processed in DSC (TGA/DSC1 Module, METLER TOLEDO (Thailand) Co., Ltd.) in non isothermal mode, under condition of nitrogen gas at flow rate about 50 mg/min. In the first heating step, the temperature would increase from 0°C to 190°C with heating rate about 3°C/minutes. Then, specimen was cooled down from 190°C to 0°C with the same rate. In the second heating step, specimen was heated from 0°C to 190°C with the same rate.

The degree of crystallinity (χ_c) of PLA in compound can be determined by using Eq. (2):

$$\chi_c(\%) = \frac{\Delta H_m}{\Delta H^0} \times \frac{1}{x_{PLA}} \times 100\% \qquad (2)$$

Where ΔH_m is the heat of fusion of sample; ΔH^0 is the heat of fusion for 100% crystalline material that is 93 J/g[3]; x_{PLA} is weight ratio of PLA in compound.

Mechanical Property Investigation

The dumbbell shaped specimens of the samples was cut by Laser cutting (6040N) according to DIE C, ASTM D 412. The tensile testing was performed at a crosshead speed of 50 mm/minutes. At least 10 specimens were tested and the average values were reported. The instrument used was Universal Testing Machine model 5960 Series, INSTRON (USA).

Results and Discussion

Cure characteristics of ENR Compound

After mixing, ENR compound was examined for cure characteristics. Figure 1 (a) shows the effect of organic modifier of OMMT on scorch time. It was found that C30B prolonged the scorch time of rubber compound. On the other hand, the other types of organic modified MMT, C15A and C20A cause the shortening of scorch time.

It was explained elsewhere that some organic modifiers could act as catalyst and therefore reduce both cure and scorch times.[4] In addition, amine group of the organic modifier could promote proficiently crosslinking reaction.[5] It was possible that the good interaction between amine group on organoclay galleries and hydroxyl group in phenolic resin could also occur. Similar results were reported by Sunil P. Lonkar et al.[6] It was not the case for Ali sanadi and coworkers[7] who reported that the addition of organoclay into butyl rubber cured with phenolic resin increased scorch time and cure time. They explained that the amine group of clay modifier obstructed reactivity of curing agents. It could be notable that the rubber used in the particular work was non-polar rubber. Furthermore, diffusion of curing agents was also an important factor. If curing agents is difficult to diffuse, crosslinking reaction would be sluggish due to the obstruction of organoclay. Especially MMT was modified by surfactants containing hydroxyl group such as C30B which could increase scorch time of rubber compound.

The effect of OMMT on cure time is shown in Figure 1 (b). It was found that C15A and C20A could delay cure time. Similar reason was described for scorch time in the previous section. In contrast, C30B reduced cure time and the cure time increased with increasing OMMT content. This may be attributed to the molecule of the organic modifier in C30B, which is methyl tallow bis-2-hydroxyethyl quaternary ammonium which could act as accelerator. Similar result was found in polychloroprene system.[7] However, the cure time was found slightly change upon the C30B contents.

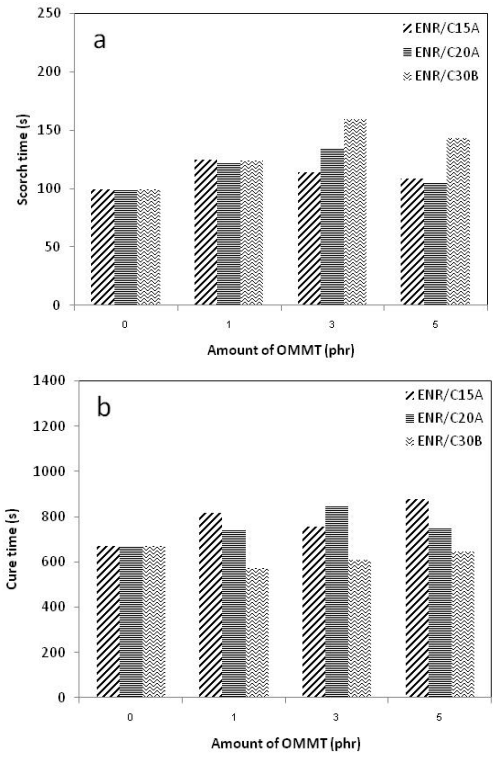

Figure 1. Effect of types of OMMT on (a) scorch time and (b) cure time of ENR compound (The displayed amount of OMMT in figure was real amount of OMMT after TPV was prepare completely.)

Morphology of OMMT-PLA/ENR TPV

XRD Characterization

Structure and dispersion of reinforcing agent in polymer composites are very important factors because they affected properties of composites directly. Therefore, structure and dispersion of composites reinforced with organoclay need to be characterized by XRD to study d_{001}-spacing of organoclay. A number of researches[8-10] reported that d_{001}-spacing of C15A, C20A and C30B were 3.15, 2.42 and 1.85 nm respectively. XRD patterns of TPVs reinforced with OMMT are shown in Figure 2. It is noted that XRD patterns of the blends reinforced with 5 phr of C15A and C20A show two similar peaks. The first peak locates at $2\theta = 2.4°$ related to

d_{001}-spacing about 3.68 nm. The increase of d-spacing of the layers resulted from the polymer chain could be able to insert into clay galleries to form intercalated structure of nanocomposite.[11-13] The second peak located at 2θ = 4.8° related to d-spacing about 1.84 nm. This represented collapse of clay galleries.[13] Composite reinforced with 5 phr of C30B also shows two peaks on XRD pattern. The first peak locates at 2θ = 2.3° related to d_{001}-spacing about 3.84 nm. This also indicated intercalated structure of nanocomposite.[11-13] The second peak located at 2θ = 5.1° related to d-spacing about 1.73 nm. The low intensity of the second peak of C30B shows a little collapse of clay galleries.

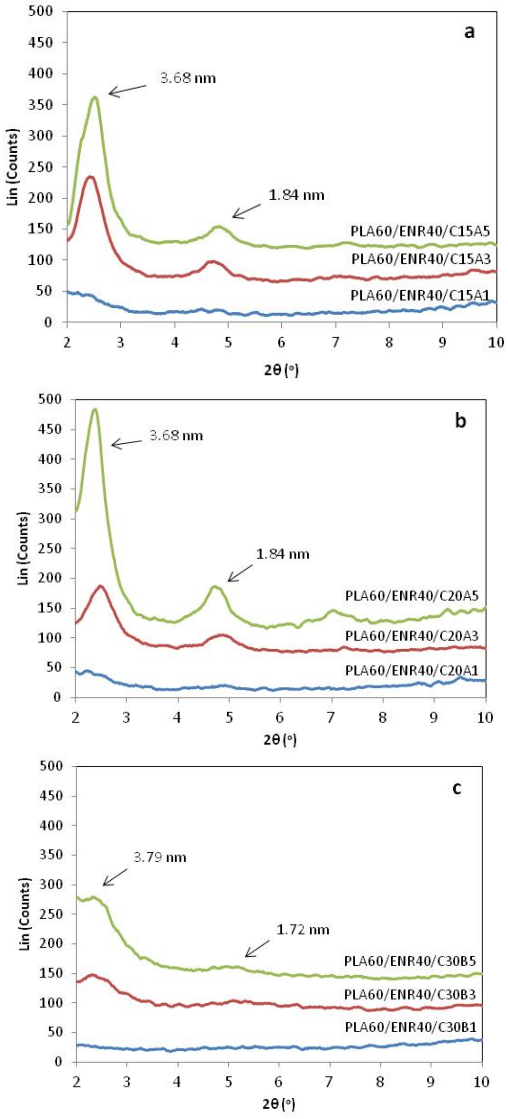

Figure 2. XRD patterns of (a) PLA/ENR/C15A, (b) PLA/ENR/C20A and (c) PLA/ENR/C30B

SEM Micrographs

SEM micrographs of cryogenic fractured surfaces of TPVs filled with 1 phr of C15A and C20A are shown in Figures 3 (b) and (e), respectively. Each figure exhibits rough surface due to plastic deformation of polymer matrices during fracturing. SEM micrographs of TPVs filled with 3 and 5 phr of C15A are shown in Figure. 3 (c) and (d) and those of C20A are shown in Figures 3 (f) and (g), respectively. These results show less rough surface than the ones containing less OMMT. The morphology of the particular fractured surface was similar to that of TPV without OMMT (Figure 3 (a)). It was noticeable that there were no clay platelet and phase separation on fractured surface of all specimens. Figures 3 (h), (i) and (j) show fractured surface of TPVs filled with different contents of C30B. It revealed smooth fractured surface at 1 phr of C30B and rough fractured surface at 3 and 5 phr of C30B due to plastic deformation during specimen fracture. For all contents of C30B, there were no clay platelet and phase separation found on fractured surface.

Fractured surface from tensile tested TPVs specimen without OMMT is shown in Figure 4 (a). It revealed the plastic deformation and some cavity due to the failure under tension. Fractured surface of tensile tested specimens of TPVs filled with 1 phr of C15A is shown in Figure 4 (b). Plastic deformation and cavity occurred due to the stretching of rubber phase. This phenomenon is similar to the TPV without OMMT. At the content of C15A of 3 and 5 phr in TPVs, shown in Figures 4 (c) and (d), it can be observed that fractured surface did not show much plastic deformation. This could be explained that the large content of OMMT could struggle molecular slippage during tension.

Fractured surface of tensile tested TPVs filled with 1 phr of C20A displays large and long stretched plates due to plastic deformation during tensioning, as can be seen in Figure 4 (e). The length and size of stretched plates decreased and the fractured surface were more smooth when OMMT content increased as shown in Figures 4 (f) and (g). Fractured surface of tensile tested TPVs filled with 1 phr of C30B, as shown in Figure 4 (h), displays surface characteristic similar to TPVs without OMMT but less elongated sheet at the surface. This could be due to the brittleness of PLA phase. At the C30B content of 3 phr, Figure 4 (i), some part of plastic deformation of PLA could be noticed. This could be because there is interaction between PLA and ENR that could induce plastic deformation of PLA. The plastic deformation was intense, for C30B filled TPV, when content of OMMT were at 5 phr, as shown in Figure 4 (j). This is caused by the inter-penetration of ENR and PLA and results in ductile deformation behavior.

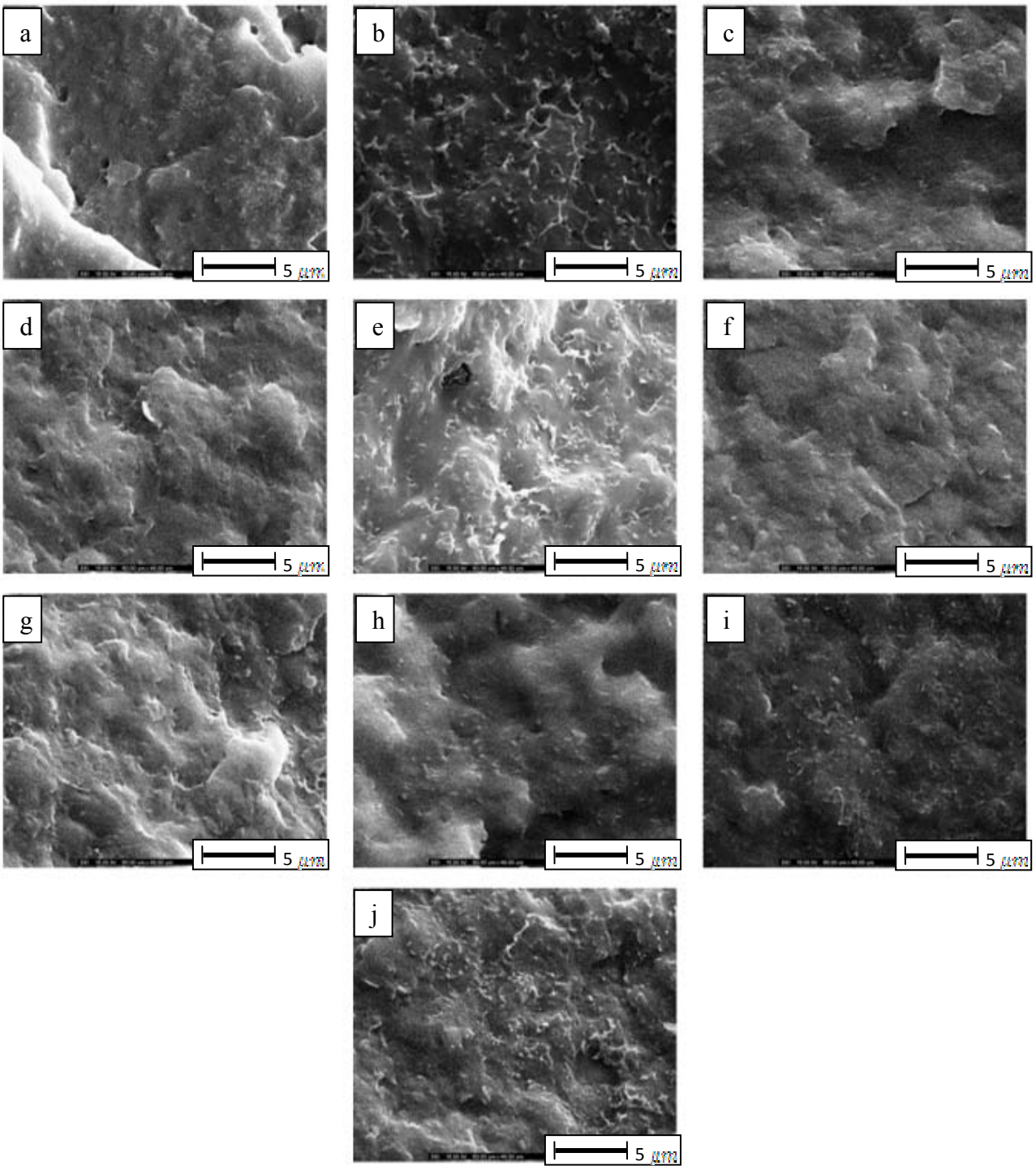

Figure 3. SEM micrographs of cryogenic fractured surface of (a) PLA60/ENR40, (b) PLA60/ENR40/C15A1, (c) PLA60/ENR40/C15A3, (d) PLA60/ENR40/C15A5, (e) PLA60/ENR40/C20A1, (f) PLA60/ ENR40/ C20A3, (g) PLA60/ENR40/C20A5, (h) PLA60/ENR40/C30B1, (i) PLA60/ENR40/C30B3 and (j) PLA60/ ENR40/C30B5(2,000X magnification)

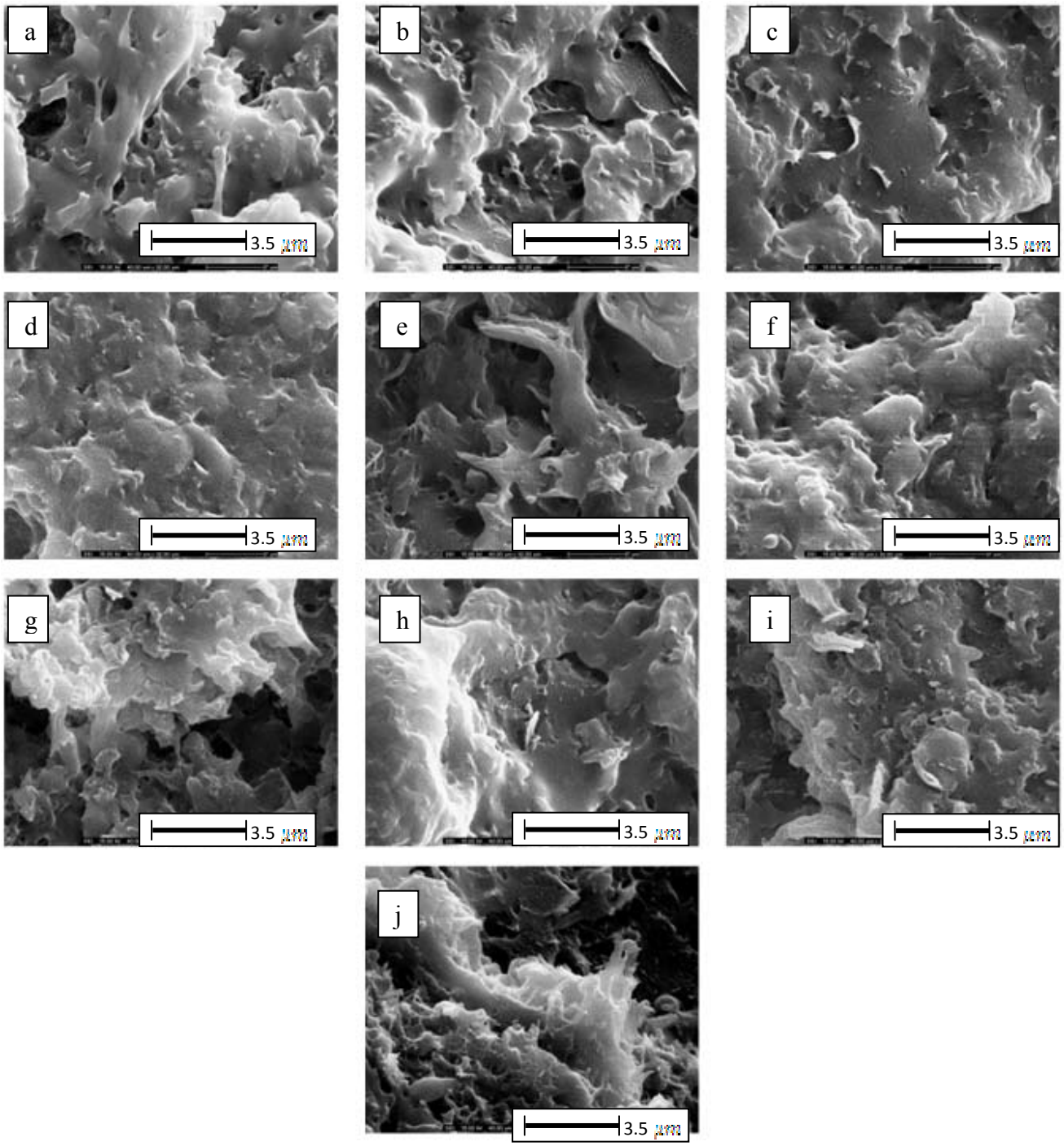

Figure 4. SEM micrographs of the fractured surface of tensile tested specimens (a) PLA60/ENR40, (b) PLA60/ENR40/C15A1, (c) PLA60/ENR40/C15A3, (d) PLA60/ENR40/C15A5, (e) PLA60/ENR40/C20A1, (f) PLA60/ENR40/C20A3, (g) PLA60/ENR40/C20A5, (h) PLA60/ENR40/C30B1, (i) PLA60/ENR40/C30B3 and (j) PLA60/ENR40/C30B5(3,000X magnification)

Mechanical Properties

Stress-strain curve of TPVs filled with OMMT, shown in Figure 5, represents the decrease of toughness after OMMT loading. However, stress-strain curves of all TPV systems showed yield point and whitening zone, shown in Figure 6. Although the whitening zone was not clearly observed for the TPV filled with high OMMT content, i.e. 5 phr.

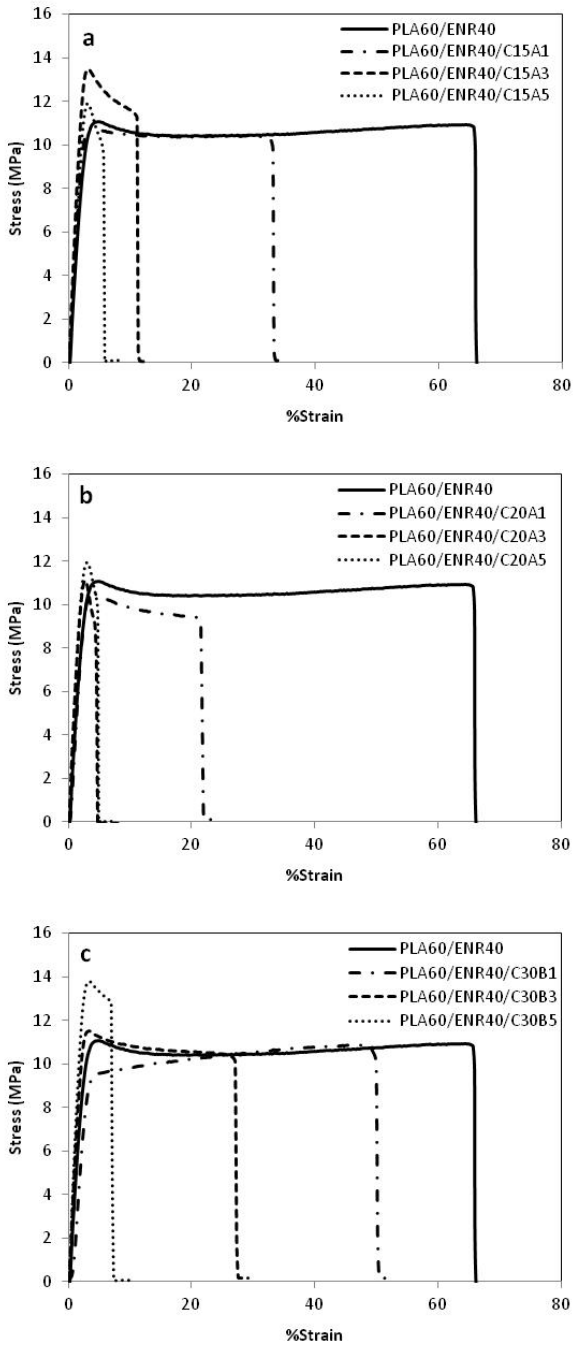

Figure 5. Stress-strain curves of (a) PLA60/ENR40/ C15A (b) PLA60/ENR40/C20A and (c) PLA 60/ENR40/C30B

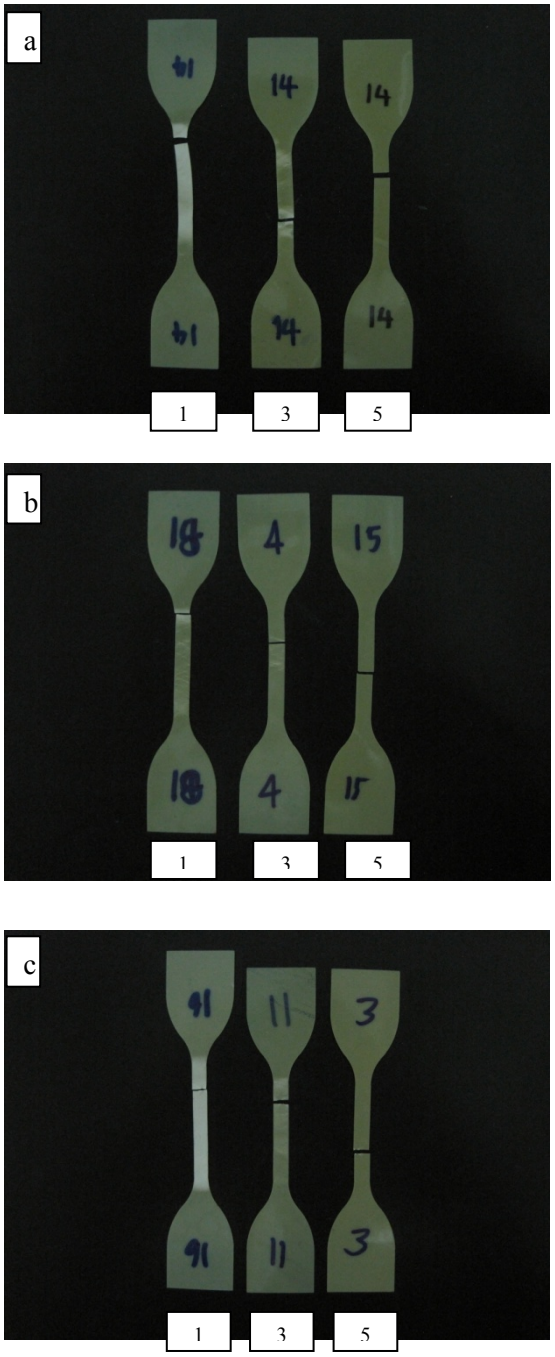

Figure 6. Tensile tested specimens of TPVs reinforced with (a) C15A, (b) C20A and (c) C30B

It was shown that there was strain softening after yielding at all contents for C15A and C20A. Only strain hardening behavior was found for TPV containing 1 phr of C30B. With the same OMMT content, TPVs filled with C15A seems to display plastic deformation region more than TPVs with C20A.

Considering the mechanical properties of TPV composites, shown in Figure 7, it was found that reinforcement with organoclay can improve tensile strength but the elongation at break is reduced with

the increase of organoclay content. These results were due to reinforcement and stiffness of organoclay.[14-16] It was noted that 5 phr of C30B could increase maximally tensile strength and modulus but elongation at break dropped less than reinforcement with other organoclays.

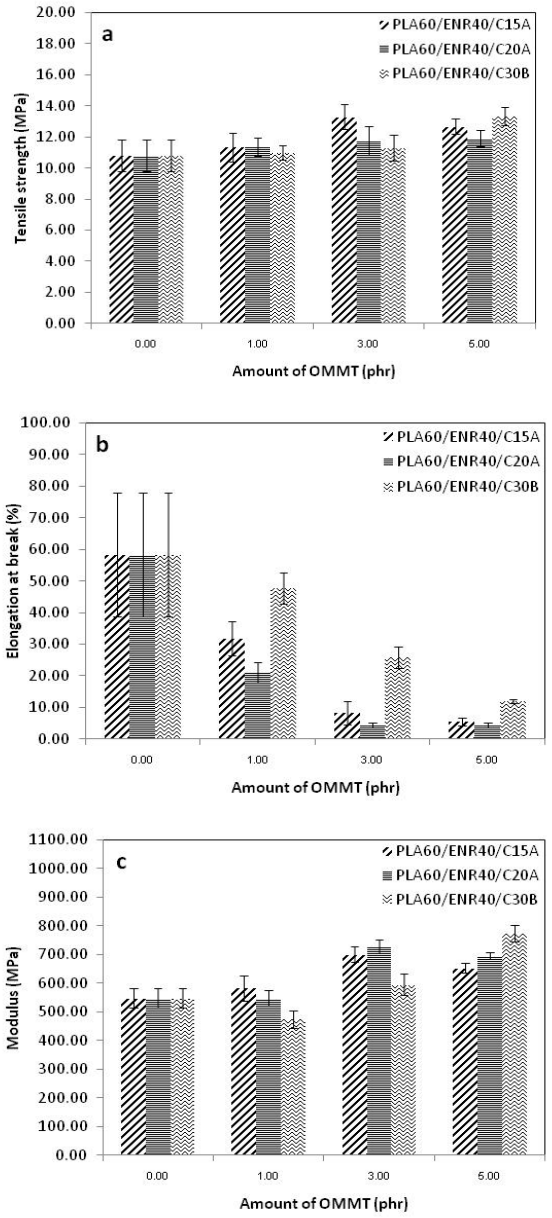

Figure 7. Effect of types and amount of OMMT on mechanical properties of OMMT-PLA/ENR TPV: (a) tensile strength; (b) elongation at break; and (c) modulus

Thermal Properties of OMMT-PLA/ ENR TPV

Crystallization and Melting characteristic of PLA in TPV

DSC thermograms of composites in the first heating step are demonstrated in Figures 8, 9 and 10. Results revealed that pure PLA, PLA60/ENR40 and TPVs reinforced with 1, 3 and 5 phr of OMMT displayed endothermic peak located at glass transition temperature. This result was due to relaxation of PLA chains.[17] The glass transition temperatures (T_g) of PLA in TPVs both with and without OMMT were close as presented in Table 1. In contrast, T_g values of PLA in TPVs both with and without OMMT were lower than that of the pure PLA about 4-5°C due to partial miscibility between PLA and ENR. Exothermic cold crystallization peak of TPVs filled with OMMT was sharper than TPVs without OMMT and cold crystallization temperature (T_{cc}) was lower than TPVs without OMMT. It was noted that both ENR and OMMT could act as nucleating agent that resulted in the increase of crystallinity of PLA. Considering of endothermic melting peak, it was found that the peak split into two peaks due to the perfect of crystallization and the difference of crystalline structures.[3, 18, 19]

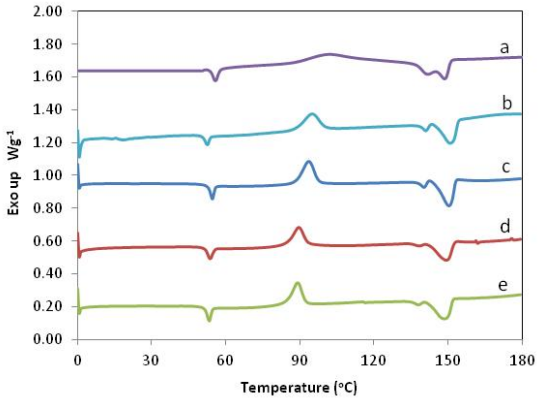

Figure 8. DSC thermogram in the first heating step of TPVs after compression molding: (a) pure PLA, (b) PLA60/ENR40, (c) PLA60/ENR40 C15A1, (d) PLA60/ENR40/C15A3 and (e) PLA60/ENR40/C15A5

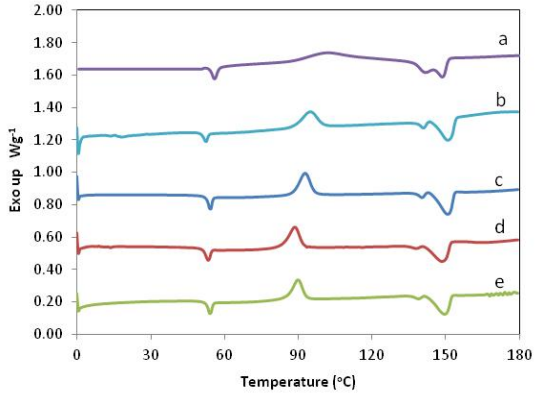

Figure 9. DSC thermogram in the first heating step of TPVs after compression molding:(a) pure PLA, (b) PLA60/ENR40, (c) PLA60/ENR40/ C20A1, (d)PLA60/ENR40/C20A3and (e) PLA 60/ENR40/C20A5

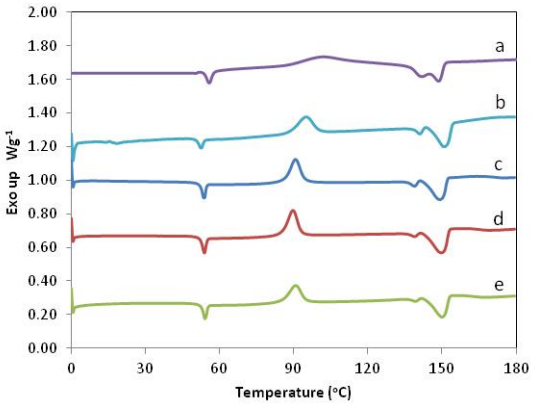

Figure 10. DSC thermogram in the first heating step of TPVs after compression molding:(a) pure PLA, (b) PLA60/ENR40, (c) PLA60/ ENR 40/C30B1, (d) PLA60/ENR40/C30B3 and (e) PLA60/ENR40/C30B5

Melting temperature (T_m) of pure PLA and TPVs both filled OMMT and unfilled OMMT were not quite different. Crystallinity of PLA in TPVs in the first heating step was presented in Table 1. It was found that TPVs filled OMMT and without OMMT showed higher crystallinity than pure PLA. These results were due to the behavior like nucleating agent of ENR. The presence of OMMT could urge the crystallization of PLA, considering from the lower T_{cc} of PLA in OMMT filled TPVs, compared to the unfilled TPV.

Table 1. Thermal properties and crystallinity in the first heating step of OMMT-PLA/ENR TPV after compression milding

Sample	T_g(°C)	T_{cc}(°C)	T_{m1}(°C)	T_{m2}(°C)	%Crystallinity
pure PLA	55.93	101.77	141.91	148.75	27.24
PLA60/ENR40	50.16	94.99	141.01	150.99	38.87
PLA60/ENR40/C15A1	51.00	93.55	140.36	150.48	29.80
PLA60/ENR40/C15A3	50.17	89.65	138.37	149.35	28.69
PLA60/ENR40/C15A5	49.79	89.05	138.00	148.50	32.83
PLA60/ENR40/C20A1	51.09	92.80	140.46	150.83	30.63
PLA60/ENR40/C20A3	50.21	88.70	139.00	148.64	31.65
PLA60/ENR40/C20A5	50.96	89.91	139.08	149.70	25.57
PLA60/ENR40/C30B1	50.85	90.60	139.00	149.14	31.11
PLA60/ENR40/C30B3	50.63	89.65	138.92	149.89	31.72
PLA60/ENR40/C30A5	50.93	90.69	140.00	150.05	27.74

The prior studies found that crystallization peaks of pure PLA and all recipes of TPVs by DSC characterization did not appear in the cooling step since crystallization of PLA was inert in cooling step.[3] However, OMMT filled TPVs was found to show exothermic peak with rather small and broad in range of 85 - 95°C on cooling step, Figure 11. Crystallization behavior of PLA in OMMT filled TPVs explained that OMMT could act as nucleating agent to ease the crystallization of PLA in the cooling step. However, there was crystallization occurring in cooling step. The crystallization temperature (T_c) and crystallinity in cooling step of TPVs with filled OMMT were presented in Table 2.

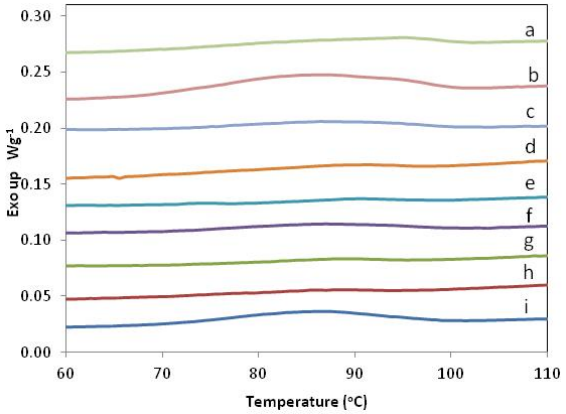

Figure 11. DSC thermogram in the cooling step of TPVs after compression molding (a) PLA 60/ENR40/C30B5, (b) PLA60/ENR40/ C30 B3, (c) PLA60/ENR40/C30B1, (d) PLA60/ ENR40/C20A5, (e) PLA60/ENR40/C20A3, (f) PLA60/ENR40/C20A1, (g) PLA60/ENR 40/C15A5, (h) PLA60/ENR40/C15A3, (i) PLA60/ENR40/C15A1

Table 2. Thermal properties and crystallinity in the cooling step of OMMT-PLA/ENR TPB after compression molding

Sample	T_c(°C)	%Crystallinity
PLA60/ENR40/C15A1	86.03	6.43
PLA60/ENR40/C15A3	85.67	0.95
PLA60/ENR40/C15A5	87.87	1.11
PLA60/ENR40/C20A1	86.88	3.28
PLA60/ENR40/C20A3	89.67	0.95
PLA60/ENR40/C20A5	87.73	2.33
PLA60/ENR40/C30B1	86.27	3.71
PLA60/ENR40/C30B3	85.88	11.59
PLA60/ENR40/C30A5	94.87	4.70

In the second heating step of OMMT-PLA/ ENR TPV after compression molding (represented in Figure 12, 13 and 14), it was found that there was no endothermic peaks located at T_g which indicated the complete polymer chain relaxation.

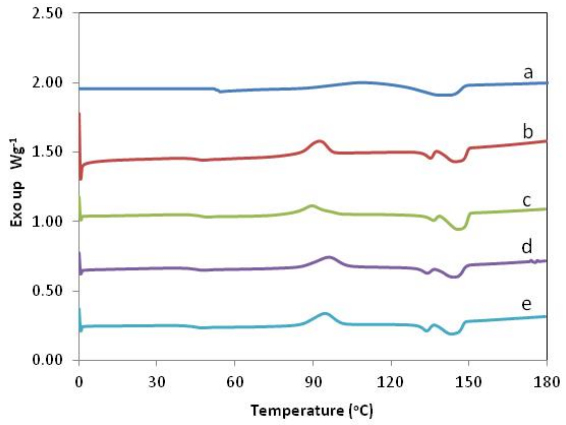

Figure 12. DSC thermogram in the second heating step of TPVs after compression molding:(a) pure PLA, (b) PLA60/ENR40, (c) PLA60/ENR 40/C15A1, (d) PLA60/ ENR40/C15A3 and (e) PLA60/ENR40/C15A5

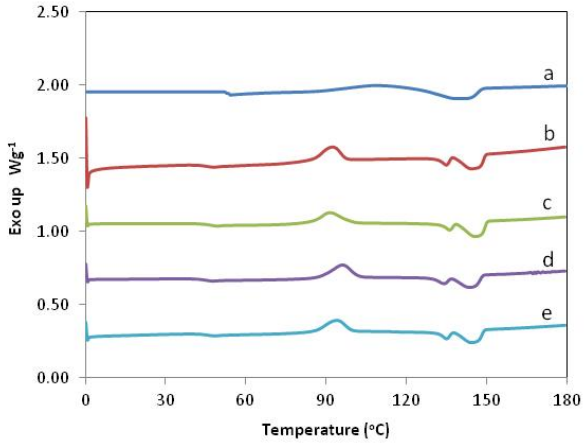

Figure 13. DSC thermogram in the second heating step of TPVs after compression molding: (a)pure PLA, (b) PLA60/ENR40, (c) PLA60/ENR 40/C20A1, (d) PLA60/ENR40/C20A3 and (e) PLA60/ENR40/C20A5

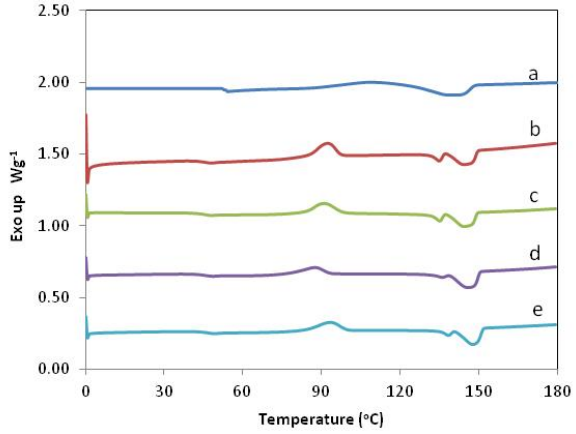

Figure 14. DSC thermogram in the second heating step of TPVs after compression molding:(a) pure PLA, (b) PLA60/ENR40, (c)PLA60/ENR 40/C30B1, (d) PLA60/ENR40/C30B3 and (e) PLA60/ENR40/C30B5

T_g values of both OMMT filled and unfilled TPVs were lower, compared with the first heating step. It could be explained that PLA molecular chains could be quite flexible. The better movement of these chains may be due to rearrangement of PLA on rubber phase.

Neat PLA exhibited the broad cold crystallization peak on the second heating scan. On the other hand, both filled and unfilled TPVs displayed sharper cold crystallization peaks. T_{cc}, presented in Table 3, of TPVs with and without OMMT, were found to shift to higher temperature. This could be explained by the thermal relaxation after the first heating and also the reforming crystalline structure could occur upon the first heating.[19] However, both melting temperatures were shifted to lower temperature which could be explained either by the relaxation or the degraded PLA induced the PLA chain to be able to pack.

Table 3. Thermal properties and crystallinity in the second heating step of OMMT-PLA/ENR TPV after compression molding

Sample	T_g(°C)	T_{cc}(°C)	T_{m1}(°C)	T_{m2}(°C)	%Crystallinity
pure PLA		108.06	142.12	142.12	20.92
PLA60/ENR40	44.74	92.29	135.06	144.55	36.54
PLA60/ENR40/C15A1	46.00	89.53	137.00	146.03	43.12
PLA60/ENR40/C15A3	43.87	96.04	134.01	144.40	41.94
PLA60/ENR40/C15A5	43.20	94.69	135.00	143.46	35.95
PLA60/ENR40/C20A1	45.35	91.43	136.00	145.89	39.21
PLA60/ENR40/C20A3	43.48	96.04	135.00	143.80	35.59
PLA60/ENR40/C20A5	44.72	93.90	136.00	144.56	35.39
PLA60/ENR40/C30B1	45.31	90.83	137.50	144.49	38.19
PLA60/ENR40/C30B3	44.31	87.38	137.00	149.24	52.33
PLA60/ENR40/C30A5	45.05	93.29	139.50	147.80	37.33

In the second heating step, it was also found that crystallinity of all TPVs filled with OMMT considerably increased, compared with crystallinity in the first heating step. The better movement of PLA's chains owing to the rearrangement related to the decrease of T_g. The better movement of molecular chain promoted crystallization of PLA.[20] Moreover, OMMT behaved as nucleating agent and promoted crystallization of PLA.

Thermal Stabilities of OMMT-PLA/ ENR TPVs

From TGA characterization, it was found that the initial thermal decomposition temperature (onset temperature) of PLA was 327°C and there was only one step of the decomposition. The decomposition temperature (T_d) was 361°C. PLA60/ENR40 had onset decomposition temperature at 287°C and there were

two stages of decomposition. The first stage was the decomposition of PLA with the T_d of 327°C and the second stage was the decomposition of ENR with T_d of 423°C. The decreased thermal stability of TPVs may be due to existing hydroxyl group in ENR molecules that occurred during the crosslinking reaction.(2) Nik Zulkepli Niriman and Hanafi Ismail(22) found that hydroxyl group in ENR molecules decomposed about 220-330°C and gave the product as hydroxyl volatile gas which could promote chain scission reaction of polyester molecules.(23) This affected negatively the thermal stability of PLA.

Thermal decomposition behavior of TPVs filled with different amounts of C15A (Figure 15) exhibits that the thermal decomposition of the TPV filled with 1 phr of C15A was quite like that of the TPV without OMMT. There were two stages of decomposition: the first stage was PLA decomposition and the second stage was ENR decomposition. Thermal decomposition temperature of the two stages slightly increased in the presence of OMMT (Table 4).

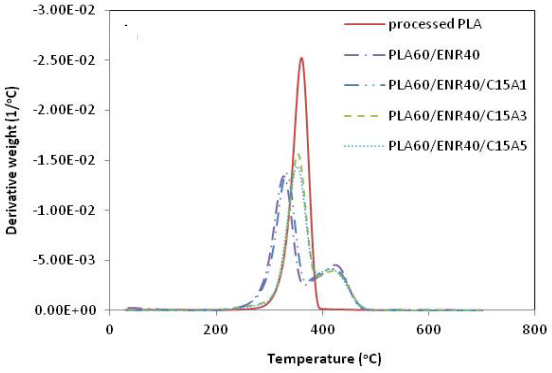

Figure 15. Thermal decomposition with the DTG weight loss curves of PLA60/ENR40/ C15A

Table 4. Thermal decomposition of OMMT-PLA/ENR TPV

Sample	T_{onset}(°C)	T_d(°C)	residue(%wt)
processed PLA	327.13	360.64	0.00%
ENR phenolic cure	342.14	414.85	1.03%
PLA60/ENR40	286.89	326.76, 423.29	0.63%
PLA60/ENR40/C15A1	292.31	332.13, 417.61	0.21%
PLA60/ENR40/C15A3	316.59	353.71, 418.92	1.61%
PLA60/ENR40/C15A5	313.3	352.66, 415.08	3.86%
PLA60/ENR40/C20A1	292.67	331.15,,420.02	0.78%
PLA60/ENR40/C20A3	315.35	351.67, 422.00	1.11%
PLA60/ENR40/C20A5	316.94	354.10, 413.06	2.82%
PLA60/ENR40/C30B1	294.49	333.70, 418.90	0.19%
PLA60/ENR40/C30B3	315.33	350.54, 416.22	1.65%
PLA60/ENR40/C30A5	320.93	355.42, 409.11	3.82%

With increasing amount of C15A to 3 and 5 phr, it was found that the first stage of thermal decomposition was similar with processed PLA. The second stage of thermal decomposition was similar with the second stage of thermal decomposition of TPVs without filled OMMT and char residue increased with amount of OMMT.

Thermal decomposition behaviors of TPVs filled with C20A and C30B were represented in Figures 16 and 17, respectively. It was found that thermal decomposition depended on the amount of OMMT like TPVs filled with OMMT type C15A. It was noted that different types of OMMT did not affect thermal decomposition behaviors of TPVs composites.

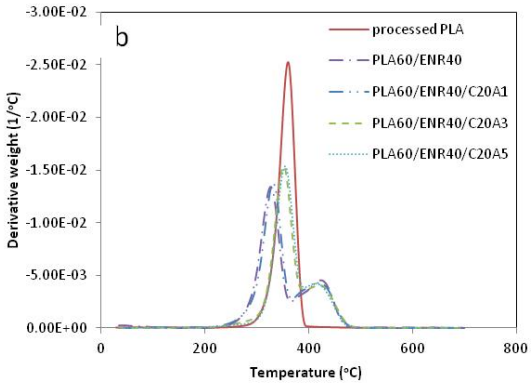

Figure 16. Thermal decomposition with the DTG weight loss curves of PLA60/ENR40/C20A

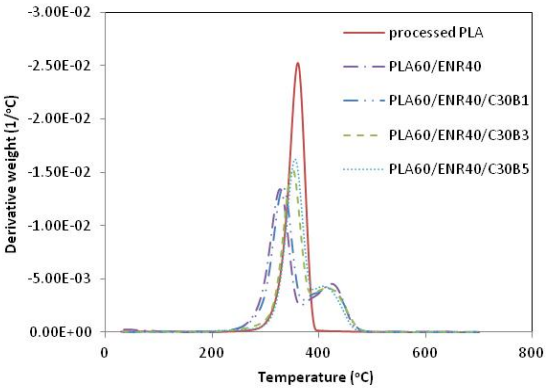

Figure 17. Thermal decomposition with the DTG weight loss curves of PLA60/ENR40/C30B

Considering the effects of OMMT, it was seen that OMMT improved thermal stability of TPVs. The more content of OMMT, the more thermal stability of TPVs increased. This was due to silicate layers of clays acted as heat barrier for polymer matrix and supported char residue process during thermal decomposition of polymer.(24) However, it was seen that T_d in the second stage of thermal decomposition decreased when the amount of

OMMT increased. This was due to clays can absorb thermal energy within clays layers and acted as a resource of thermal energy in polymer matrix under high temperature system combined with thermal energy from external system. These also could accelerate thermal decomposition of polymer.[24]

Conclusions

Tensile strength and modulus of TPVs reinforced with organoclay increased whereas elongation at break decreased with increasing organoclay content. C30B at 5 phr increased maximally tensile strength and modulus but elongation at break dropped less than reinforcement with other organoclays. This result was due to the good dispersion of C30B. Morphology of freeze fractured surface did not depend on types and contents of organoclay. It was homogeneous and did not present organoclay platelet. Morphology of tensile tested specimens was dependent on types and content of organoclay. However, TPVs filled with less organoclay would display more plastic deformation compared with TPVs filled with more organoclay.

Types and content of organoclay did not affect T_g and melting behavior of PLA but they affected crystallization behavior of PLA through sharpening cold crystallization peak and reducing cold crystallization temperature. In addition, there was a small exothermic peak during cooling. These increased crystallinity of PLA in TPVs. All types of organoclay could improve thermal stabilities of TPVs similarly. Especially, the presence of 3 and 5 phr of organoclay could compensate for lost thermal stabilities of TPVs satisfactorily.

Acknowledgements

We would like to thank the Department of Materials Science and Engineering, Faculty of Engineering and Industrial Technology, Silpakorn University, Nakornpathom, for their support and sincere thank to the Prince of Songkla University for phenolic resin support.

Reference

1. Thitithammawong, A., Nakason, C., Sahakaro, K. and Noordermeer, J.W.M. (2007). Thermoplastic vulcanizates based on epoxidized natural rubber/poly propylene blends: Selection of optimal peroxide type and concentration in relation in relation to mixing conditions. *Eur. Polym. J.* **43** : 4008-4018.

2. Dai, J. C. and Huang, J. T. (1999). Surface modification of clays and clay-rubber composite. *Appl. Clay Sci.* **15** : 51-65.

3. Tsai, C. C., Wu, R. J., Cheng, H. Y., Li, S. -C., Siao, Y. -Y., Kong, D. C. and Jang, G.-W. (2010). Crystallinity and dimensional stability of biaxial oriented poly(lactic acid) films. *Polym. Degrad. Stab.* 95 : 1292-1298.

4. Avalos, F., Ortiz, J. C., Zitzumbo, R., López-Manchado, M. A., Verdejo, R., and Arroyo, M. (2008). Effect of montmorillonite intercalant structure on the cure parameters of natural rubber. *Eur. Polym. J.* 44 : 3108-3115.

5. Teh, P. L., Ishak, Z. A. M., Ishiaku, U. S. and Karger-Kocsis, J. (2003). Cure characteristics and mechanical properties of natural rubber/ organoclay nanocomposites. *J. Teknologi 39* : 1-10.

6. Lonkar, S. P., Kumar, A. P. and Singh, R. P. (2007). Photo-stabilization of EPDM–clay nanocomposites: effect of antioxidant on the preparation and durability. *Polym. Adv. Technol.* **18** : 891-900.

7. Samadi, A. and Kashani, M. R. (2010). Effects of organo-clay modifier on physical–mechanical properties of butyl-based rubber nano-composites. *J. Appl. Polym. Sci.* **116** : 2101-2109.

8. Southern Clay Products, I. Cloisite® 15A Typical Physical Properties Bulletin, *http://www.scprod.com /produ ct_bulletins/PB%20Cloisite%2015A. pdf. Accessed date: 03 June 2012.*

9. Southern Clay Products, I. Cloisite® 20A Typical Physical Properties Bulletin. *http://www.scprod.com /produ ct_bulletins/PB%20Cloisite%2020A. pdf. Accessed date: 03 June 2012*.

10. Southern Clay Products, I. Cloisite® 30B Typical Physical Properties Bulletin. *http://www.scprod.com /produ ct_bulletins/PB%20Cloisite%2030B. pdf. Accessed date: 03 June 2012*.

11. Kumar, M., Mohanty, S., Nayak, S. K. and Parvaiz, M. R. (2010). Effect of glycidyl methacrylate (GMA) on the thermal, mechanical and morphological property of biodegradable PLA/PBAT blend and its nanocomposites. *Bioresour. Technol.* **101** : 8406-8415.

12. Thipmanee, R., Magaraphan, R. and Nampitch, T. *Mechanical properties and morphology of poly(lactic acid) (PLA)/epoxidized natural rubber (ENR)/organoclay nanocomposites*. Kasetsart University.

13 Najafi, N., Heuzey, M. C. and Carreau, P. J. (2012) Polylactide (PLA)-clay nanocomposites prepared by melt compounding in the presence of a chain extender. *Comp. Sci. Technol.* **72** : 608-615.

14. Leu, Y. Y., Ishak, Z. A. M. and Chow, W. S. (2012). Mechanical, thermal, and morpholo gical properties of injection molded poly (lactic acid)/SEBS-g-MAH/organo-montmorillonite Nanocomposites. *J. Appl. Polym. Sci.* **124** : 1200-1207.

15. Wang, X., Jia, D. and Chen, M. (2008). Structure and properties of epoxidized nature rubber/ organoclay nanocomposites, In : *IEEE International Nanoelectronics Conference. 2008.*

16. Balakrishnan, H., Hassan, A., Wahit, M. U., Yussuf, A. A. and Razak, S. B. A. (2010). Novel toughened polylactic acid nanocomposite: Mechanical, thermal and morphological properties. *Mater. Design.* **31** : 3289-3298.

17. Thellen, C., Orroth, C., Froio, D., Ziegler, D., Lucciarini, J., Farrell, R., D'Souza, N. A. and Ratto, J. A. (2005). Influence of montmorillonite layered silicate on plasticized poly(L-lactide) blown films. *Polymer* **46** : 11716-11727.

18. Fukushima, K., Tabuani, D., Camino, G. (2009). Nanocomposites of PLA and PCL based on montmorillonite and sepiolite. *Mater. Sci. Eng.* **29** : 1433-1441.

19. Picard, E., Espuche, E., Fulchiron, R. (2011). Effect of an organo-modified montmorillonite on PLA crystallization and gas barrier properties. *Appl. Clay Sci.* **53** : 58-65.

20. Li, H., Huneault, M. A. (2007). Effect of nucleation and plasticization on the crystallization of poly(lactic acid). *Polymer*. **87** : 6855-6866.

21. Noriman, N. Z., Ismail, H., Rashid, A. A. (210). Characterization of styrene butadiene rubber/ recycled acrylonitrile-butadiene rubber (SBR/ NBRr) blends: The effects of epoxidized natural rubber (ENR-50) as a compatibilizers. *Polym. Test.* **29** : 200-208.

22. Noriman, N. Z., Ismail, H. (2012). Effect of epoxidized natural rubber on thermal properties, fatigue life, and natural weathering test of styrene butadiene rubber/recycled acrylonitrile-butadiene rubber (SBR/NBRr) blends. *J. Appl. Polym. Sci.* **123** : 779-787.

23. Liu, X., Khor, S., Petinakis, E., Yu, L., Simon, G., Dean, K., Bateman, S. (2010). Effects of hydrophilic fillers on the thermal degradation of poly(lactic acid). *Thermochimica Acta*. **509** : 147-151.

24. Chow, W. S., Lok, S. K. (2009). Thermal properties of poly(lactic acid)/organo-montmorillonite nanocomposites. *J.Therm. Anal. .Colorim.* **95** : 627-632.